A Consideration on Generation Mechanism of Local Earthquakes

AUTHOR(S):

Mikumo, Takeshi

CITATION:

Mikumo, Takeshi. A Consideration on Generation Mechanism of Local Earthquakes. Memoirs of the College of Science, University of Kyoto. Series A 1959, 29(2): 221-240

ISSUE DATE:

1959-09

URL:

http://hdl.handle.net/2433/257432

Memoirs of the College of Science, University of Kyoto, Series A,
Vol. XXIX, No. 2, Article 9, 1959.

A CONSIDERATION ON GENERATION MECHANISM OF LOCAL EARTHQUAKES

BY

Takeshi MIKUMO

(Received July 8, 1959)

ABSTRACT

The mechanism of occurrence of local earthquakes generated in Wakayama District was studied from the "push-pull" pattern of initial motions and the amplitude distributions of the *P*- and *S*-waves. It may safely be explainable to be of a conical type rather than a quadrant one.

A consideration on the former type of mechanism may suggest an azimuthal difference in the dimension of focal region.

1. Introduction

The study on the mechanism of earthquake occurrence, based on the distribution of dilatation and compression of seismic initial motions, may be one of the most interesting and important problems in seismology. This problem has already been studied by many seismologists and many brilliant results have been piled up. The progresses of these researches are historically reviewed by some Japanese seismologists in their elaborate papers (**1, 2**).

Nowadays, it is generally accepted, from the excellent investigations hitherto made, that there exist several kinds of types in the geographical "push-pull" distributions of the initial motions: the predominant one is a quadrant type.

This is such a case in which the "push-pull" distribution or the pattern of the initial anaseismic and kataseismic movements is divided into quadrants by two nodal planes intersecting perpendicularly at the focus. This type of distribution was found first by T. Shida in 1917 and was called "the crack-earthquake" by himself. Many seismologists paid increasing attention to his discovery and this was a first step in Japan towards the study on the mechanism of earthquakes.

According to a series of studies made especially in our country, it was ascertained theoretically that the quadrantal push-pull distribution could be caused by a couple of compressional and tensile stresses working perpendicularly at the origin (**2**), or even by a uniform shear stress resulting in a single fracture (**3**). The so-called "fault-plane" solution (**4, 5**) belongs also to this broad category.

Another case is, on the other hand, a conical type in which the nodal curves on the Earth's surface for the pattern of condensation and rarefaction of the initial motions can be expressed as a kind of conical section. The case was detected by

Tanahashi in a deep-seated earthquake in 1931. Some investigators confirmed thereafter the existence of this type, and one of them gave a first theoretical explanation to this sort of distribution. The theoretical studies on the mechanism of occurrence which causes a conical type distribution will be mentioned subsequently.

In contrast to the case of great earthquakes, we can find only a few investigations (**6, 7, 8, 9, 10**) about the generation mechanism of minor earthquakes, such as local shocks or aftershocks.

In 1954 and 1956, seismometric observations were carried out in the epicentral region of local earthquakes in Wakayama District (**11**) for the purpose of clarifying the unsolved natures of micro-earthquakes and presuming the crustal structure in the area concerned. The results obtained in these observations may be considered to have offered a clue to the above-mentioned problems.

In the present paper, the mechanism of earthquake occurrence will be studied in some detail, not only from the aspect of the push-pull pattern of initial P-waves but also from comparison of the amplitudes recorded at each station with the theoretical distribution of the amplitudes of the longitudinal and transversal waves. We shall investigate that the generation mechanism for these shocks is interpreted to be of which type stated above, and we shall make some considerations on the origin of the earthquakes.

2. Observed data

The data used in the present study are a great number of seismograms recorded in the observations in 1954 and 1956 at our six stations: Idakiso, Wakanoura, Fuyuno, Nokami, Kainan and Yoro, and several observatories of the Earthquake Research Institute of Tokyo University. All of these stations were selected so as to be situated in a metamorphic rock zone within the epicentral area of about 10 km in radius, taking Kainan City as its centre. The positions of the observation stations and the epicentres of earthquakes mentioned in this analysis were shown in the previous paper. In these observations, some ten local shocks were clearly recorded by the electromagnetic seismometers of variable reluctance type of 0.45 sec in natural period connected with the galvanometer of 0.40 sec in free period.

The push-pull distribution of initial motions in every earthquake was here studied by use of the data obtained at the respective stations. When the nodal curves were tentatively assumed to be a pair of lines (**11**), the distribution indicated a type similar to the quadrant one in the case of very shallow earthquakes (**6**). But in many cases the nodal lines do not always cross at right angles or do not intersect at the epicentre. Upon reconsidering the matter, the focal depths for most of these earthquakes were determined to be as shallow as 4~10 km, but are of comparable order with their epicentral distances. Hence, when these shocks are regarded as an earthquake analogous to the "deep-focus earthquake" in the ordinary sense, the push-pull distribution in most cases will be understandable to be a quadrant type.

A closer examination shows, however, that it can reasonably be explained to be rather of a conical type, if the previously assumed nodal curves were redetermined. Fig. 1 shows several examples of the push-pull distribution in the case of conical type.

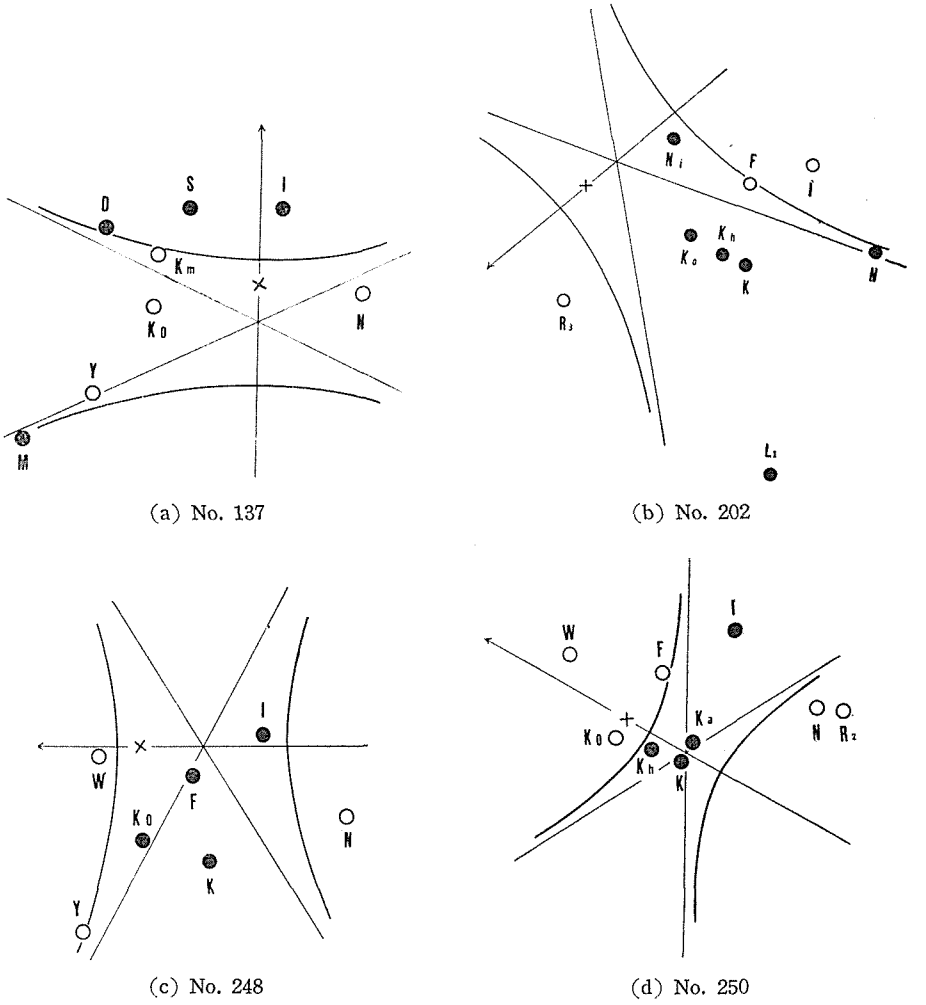

(a) No. 137 (b) No. 202

(c) No. 248 (d) No. 250

Fig. 1. Examples of push-pull distribution of initial motions.
(○: push, ●: pull)

Naturally, it is difficult to conclude solely from the push-pull pattern, without any study on the amplitude distribution of the *P*- and *S*-waves, that the mechanism of these local shocks corresponds to either type of the two. We are probably allowed, however, to suppose that the local earthquakes in this region may have a mechanism bearing a conical type distribution. For this reason, the already-made theoretical studies

will be reviewed in the next paragraph, in order to clarify in what cases this type of distribution can arise.

3. A brief review of the past theoretical studies on conical type distribution

On the mechanism with push-pull distribution of a conical type, some Japanese seismologists, such as Ishimoto, Kawasumi, Inouye, Takagi, Usami and Hirono have made theoretical studies in various cases.

M. Ishimoto (**12**) investigated practical examples of the push-pull pattern in many earthquakes and came to the conclusion that in all cases the nodal curves for distribution of the initial movements are represented by a conical section with push-sense inside. For this mechanism, he proposed such an origin-model that was composed of two zonal harmonics, $P_2(\cos\theta)$ (quadruple source) and $P_0(\cos\theta)$ (single source), which are particular solutions of the fundamental equation of propagation of spherical waves. This is the well-known hypothesis called "magma intrusion theory."

Following Ishimoto's idea, H. Kawasumi (**13**) made more detailed theoretical and practical studies. He investigated theoretically, by an excellent method, the propagation of spherical waves in a homogeneous isotropic medium, obtaining the same solution as Sezawa's (**14**). Namely, his general solutions for the equations $(\nabla^2+h^2)\phi=0$, $(\nabla^2+k^2)\psi=0$ (where $h^2=\rho p^2/(\lambda+2\mu)$, $k^2=\rho p^2/\mu$) are expressed by

$$\begin{cases} \phi=\sum_{n=0}^{\infty}\sum_{m=0}^{\infty}A_{nm}\dfrac{H^{(2)}_{n+1/2}(hr)}{\sqrt{r}}P_n^m(\cos\theta)\sin(m\varphi+\varepsilon), \\ \psi=\sum_{n=0}^{\infty}\sum_{m=0}^{\infty}B_{nm}\dfrac{H^{(2)}_{n+1/2}(kr)}{\sqrt{r}}P_n^m(\cos\theta)\sin(m\varphi+\varepsilon), \end{cases}$$

where ϕ and ψ are scalar- and vector-potentials respectively, and the displacements in all directions can be derived from these quantities. Kawasumi dealt especially with the conical type distribution corresponding to the case of $n=2$ and $m=0$ in the above solutions, and compared the observed values at each station with the theoretical amplitudes of the longitudinal and transversal waves, taking the effects due to crustal structure into consideration.

In addition, the case of $n=2$ and $m=2$ in the above or Sezawa's solution is equivalent to the type studied by Matuzawa (**15**) and Hasegawa (**16**), and the case of $n=2$ and $m=1$ to the type discussed by Honda (**17**). These cases correspond to a quadrant type.

On the other hand, W. Inouye (**18**) studied the behaviour of the dilatational waves generated from a model of seismic origin, in which the normal pressure varying periodically on the surface of spherical cavity can be represented by the sum of two zonal harmonics $P_0(\cos\theta)e^{ipt}$ and $P_2(\cos\theta)e^{ipt}$. He also elucidated that the displacement at large distances is of the conical type distribution when the wavelengths of

the longitudinal waves are of comparable order with the dimension of seismic origin.

S. Takagi (**19**) calculated theoretically the radial displacement of elastic waves emitted from the same cavity as mentioned above when the outward normal force of harmonic, aperiodic or hydrostatic type acts on a pole, two poles or equatorial plane of the source, and confirmed that the azimuthal distribution of the initial amplitudes can be expressed in most cases as a combination of $P_0(\cos\theta)$ and $P_2(\cos\theta)$, indicating a conical type.

Moreover, T. Usami and H. Hirono (**20, 21**) recently investigated the amplitude distribution of the dilatational and distortional waves generated from a prolate or oblate spheroidal cavity in an infinite elastic medium when hydrostatic pressure or a force of harmonic type is applied on the surface of the cavity. As a result of numerical calculations, it was found that at a distant point the push-pull distribution of conical type was produced in a radial displacement of P-waves in the case of certain shapes of cavity and values of wavelength.

It is to be remarked that the conical type distribution with pull-sense inside can be found in the cases treated by Usami and Takagi.

We shall now analyse our observed data referring to the above-described theories.

4. Determination of the vertical angle of nodal cone and the inclination of its polar axis from data of push-pull distribution

Now, the nodal curves on the Earth's surface in a conical type distribution are represented, in general, by a hyperbola or an ellipse. Their shape and dimension depend upon the angle of vertex of the nodal cone, the inclination of its polar axis and the depth of hypocentre. Ishimoto, Kawasumi and Minakami (**22**) suggested the possibility of determining the axial inclination of the cone or the focal depth from the form of the curves. In this case they supposed a constancy of the vertical angle of cone, but this is functionally related with the ratio of wavelength to the dimension of the origin, in the cases investigated by Usami and Inouye. Furthermore, the shapes of nodal curves are known to be of complicated styles deformed from a conical section, if the effects due to discontinuity surfaces in the crust are taken into account (**13, 22, 23**).

Here, for the sake of simplicity, the crust mentioned in this analysis is assumed to be of a uniform medium. Under this assumption, the vertical angle and axial inclination of nodal cone will be determined from data of push-pull distribution. This is attributable to a simple problem in analytical geometry. Takagi (**23**) has already studied the present problem, but more definite expressions to estimate the above unknowns can be obtained in our case.

We shall first consider an orthogonal left-hand coordinate system $x'y'z'$, taking a hypocentre (strictly, a centre of focal region) as the origin of the coordinates, the

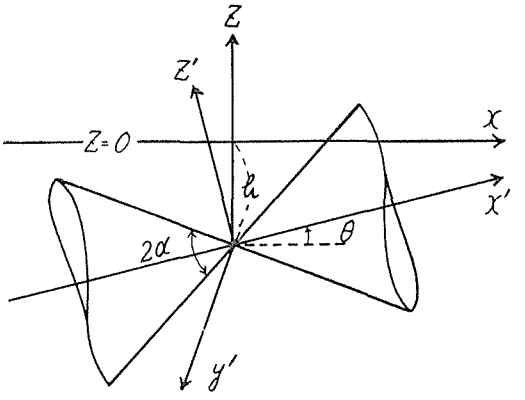

Fig. 2.

polar axis of a nodal cone as the x'-axis, and an axis parallel to the ground surface as the y'-axis (Fig. 2).

The equation of the nodal cone with the vertical angle 2α is expressed as follows:

$$-x'^2\tan^2\alpha+y'^2+z'^2=0. \quad (1)$$

Next, another coordinate system xyz having the epicentre as its origin is taken in such a way that the xy-plane coincides with the ground surface and the y-axis is parallel to y'. Then, the equation of the cone referred to the xyz-system becomes

$$(\tan^2\alpha-\tan^2\theta)x^2+2x(z+h)\sec^2\alpha\tan\theta-y^2\sec^2\theta-(1-\tan^2\alpha\tan^2\theta)(z+h)^2=0, \quad (2)$$

where θ is the angle of inclination to the ground surface and h the focal depth. The conical section on the surface can immediately be obtained by putting $z=0$ in Eq. (2). Thus,

$$(\cos 2\theta-\cos 2\alpha)x^2+2h\sin 2\theta\cdot x-(1+\cos 2\alpha)y^2=(\cos 2\theta+\cos 2\alpha)h^2. \quad (3)$$

(1) *Case of* $0\leqq\theta<\alpha$

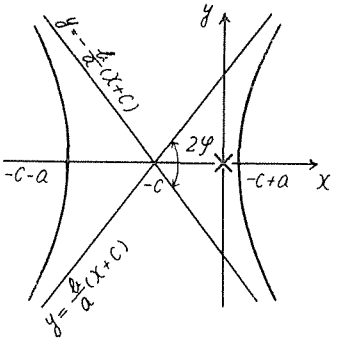

Fig. 3.

Eq. (3) can be rewritten in the form:

$$\frac{(x+c)^2}{a^2}-\frac{y^2}{b^2}=1, \quad (4)$$

where

$$\left.\begin{aligned} a^2&=\left(\frac{\sin 2\alpha}{\cos 2\theta-\cos 2\alpha}\right)^2h^2,\\ b^2&=\frac{2\sin^2\alpha}{\cos 2\theta-\cos 2\alpha}h^2,\\ c&=\frac{\sin 2\theta}{\cos 2\theta-\cos 2\alpha}h. \end{aligned}\right\} \quad (5)$$

Consequently, the nodal curve on the surface expressed by Eq. (4) is a hyperbola as shown in Fig. 3. In this case the epicentre lies on the axis of symmetry traversing the curves. Let the angle of intersection of the asymptotes of the hyperbola (4) be denoted by 2φ. Then we obtain

$$\tan^2\varphi=\left(\frac{b}{a}\right)^2=\frac{\cos 2\theta-\cos 2\alpha}{1+\cos 2\alpha}. \quad (6)$$

a) When the focal depth h, the angle of intersection of the asymptotes 2φ and

the distance c between the epicentre and the point of intersection of the asymptotes are determined from observation, we get θ and α from Eqs. (5) and (6) as:

$$\tan\theta = c\sin^2\varphi/h\,, \tag{7}$$

$$\cos\alpha = \cos\varphi\cos\theta\,. \tag{8}$$

b) When h, 2φ, and the distance a between the epicentre and the nearer vertex of the nodal curve are estimated, α and θ can be determined from the following formulae:

$$\tan\alpha = a\tan^2\varphi/h\,, \tag{9}$$

$$\cos\theta = \cos\alpha/\cos\varphi\,. \tag{8'}$$

Here, the following relationship needs to hold in the above two cases:

$$\frac{c}{a} = \frac{\sin 2\theta}{\sin 2\alpha}\,. \tag{10}$$

c) When we can determine h, c and a, α and θ can easily be obtained from Eqs. (5) and (10), as follows:

$$\tan 2\alpha = 2p/(p^2-q^2-1)\,, \tag{11}$$

$$\tan 2\theta = 2q/(p^2-q^2+1)\,, \tag{12}$$

where $p=a/h$ and $q=c/h$. In this case Eq. (8) is required to hold.

(2) Case of $\alpha<\theta\leqq\pi/2$

In this case, the nodal curve becomes an ellipse shown in Fig. 4, and α and θ can be obtained in the same way as in the former case, by determining the longer and shorter axes or their ratio and the distance between the epicentre and the centre of the ellipse.

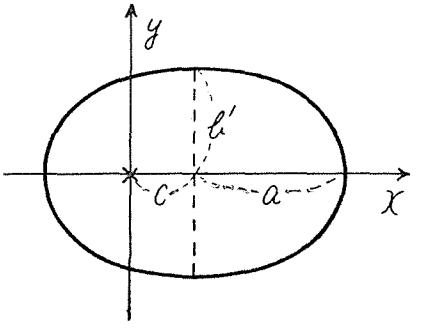

Fig. 4.

In the special case of $\theta=\alpha$ the nodal curve becomes a parabola, while in the case of $\theta=\pi/2$, it becomes a circle.

In short, the vertical angle and the axial inclination of the nodal cone can be estimated from the push-pull distribution of initial motions, by determining beforehand the focal depth by a travel-time analysis. Estimation of these quantities, however, will inevitably be attended with considerable errors, unless a sufficiently dense net of observation stations is spread over the area concerned. In our case, nodal curves in some possible extreme cases were examined and their mean values were adopted.

The results obtained by applying the above-described method to our data in 28

Table 1. Vertical angle and inclination angle of nodal cone in every earthquake.

Shock No.	h (km)	Φ_N	a (km)	c (km)	φ	α	θ
121	11.2	108° ± 19°	5.0 ± 0.7	2.2 ± 0.7	67° ± 4°	67° ± 4°	7° ± 2°
122	3.7	204 ± 15	2.0 ± 0.3	0.9 ± 0.3	63 ± 3	64 ± 4	11 ∓ 2
123	3.3	171 ± 18	2.0 ± 1.1	0.8 ∓ 0.8	59 ± 15	60 ± 16	10 ± 10
135	4.6	15 ± 12	2.7 ± 0.3	0.4 ± 0.2	61 ± 4	61 ± 4	4 ∓ 2
136	4.7	136 ± 7	4.8 ± 0.8	5.0 ∓ 0.5	53 ± 8	59 ± 8	32 ± 6
137	5.1	0 ± 2	3.0 ± 0.2	2.0 ± 0.2	62 ± 2	63 ± 2	17 ∓ 2
140	6.3	0 ± 20	3.3 ± 0.7	5.5 ± 0.7	68 ± 4	72 ± 3	35 ± 6
151	5.8	14 ± 22	2.9 ± 0.9	3.8 ∓ 0.9	67 ± 7	69 ± 10	39 ± 8
201	10.3	5 ± 30	8.0 ± 1.0	1.0 ± 1.0	52 ± 2	53 ± 3	4 ± 4
202	6.2	140 ± 5	4.0 ± 0.8	2.0 ∓ 0.9	58 ± 8	60 ± 9	14 ± 7
206	9.3	278 ± 13	5.0 ± 2.5	5.0 ± 2.5	64 ± 11	67 ± 10	24 ∓ 10
207	3.6	303 ± 28	2.9 ± 1.1	0.8 ± 1.1	58 ± 15	59 ± 15	11 ± 4
217	7.9	93 ± 3	1.4 ± 0.2	6.4 ± 0.3	81 ± 3	83 ± 2	38 ∓ 2
218	5.6	154 ± 22	2.7 ± 0.6	3.3 ∓ 0.6	66 ± 15	70 ± 13	27 ± 10
220	5.1	270 ± 11	4.4 ± 0.6	0.0 ∓ 0.5	49 ± 5	49 ± 5	0 ± 4
222	4.4	318 ± 27	3.5 ± 2.3	4.0 ± 2.5	59 ± 17	64 ± 13	31 ∓ 15
223	5.2	92 ± 11	2.1 ± 0.5	3.2 ± 0.3	69 ± 6	73 ± 5	29 ∓ 2
224	8.9	358 ± 20	3.6 ± 1.9	2.8 ± 2.0	69 ± 10	70 ± 10	15 ∓ 10
226	7.4	187 ± 8	3.4 ± 0.8	0.8 ± 0.8	65 ± 4	66 ± 3	5 ± 5
228	7.3	318 ± 23	5.8 ± 0.3	0.0 ± 3.5	52 ± 5	52 ± 3	0 ± 15
230	8.4	334 ± 3	5.0 ± 0.8	4.7 ± 0.8	61 ± 5	64 ± 3	24 ∓ 3
236	6.3	252 ± 10	4.1 ± 1.8	1.7 ± 1.7	57 ± 5	58 ± 4	11 ∓ 7
247	12.0	214 ± 20	6.0 ± 2.4	2.0 ± 2.0	64 ± 9	64 ± 7	8 ∓ 8
248	4.6	89 ± 4	4.1 ± 0.8	2.9 ± 1.5	56 ± 10	58 ± 4	24 ± 10
249	8.8	174 ± 10	3.6 ± 1.0	2.7 ± 0.8	68 ± 6	69 ± 5	20 ± 2
250	3.7	58 ± 8	2.0 ± 0.4	2.9 ± 0.6	67 ± 3	70 ± 2	33 ∓ 6
251	5.3	305 ± 33	4.0 ± 1.0	5.5 ± 0.5	61 ± 10	68 ± 10	38 ∓ 6
253	6.6	181 ± 18	4.6 ± 2.6	2.4 ± 2.4	57 ± 17	58 ± 15	14 ∓ 14

α: the vertical angle of nodal cone; θ: the inclination of polar axis of the cone; Φ_N: the axial orientation of nodal cone measured from northward.

earthquakes are tabulated in Table 1. Eqs. (11) and (12) were used in the present case. The errors in α and θ do not exceed 10° for most of the shocks.

5. Amplitude distribution in the case of conical type

In this section, the amplitude distribution will be calculated theoretically from the data listed in Table 1, and will be compared with the amplitudes observed at each station.

As reviewed in § 3, theoretical studies on various mechanisms causing the distribution of conical type have been made. In almost all the cases mentioned there, the azimuthal distribution of radial and tangential displacements at large distances, as compared with the wavelength, can exactly or approximately be expressed by a combination of spherical harmonic functions: $a_0P_0(\cos\eta)+a_2P_2(\cos\eta)$ and $bP_2^1(\cos\eta)$ respectively, with arbitrary constants a_0, a_2 and b (**12, 13, 18, 19, 20, 21**). It can safely be regarded also in Usami's model that the distribution approaches the above form with fairly good accuracy.

Hence in these cases, the radial amplitude, u, and tangential one, v, on a spherical surface with radius r can be represented by the following form in terms of the vertical angle of the nodal cone, 2α:

$$\left.\begin{aligned} u &\propto a_0P_0(\cos\eta)+a_2P_2(\cos\eta) = A\cos 2\eta+B = 2A(\cos^2\eta-\cos^2\alpha)\,, \\ v &\propto C\sin\eta\cos\eta\,, \end{aligned}\right\} \qquad (13)$$

where η is the angle measured from the polar axis.

We shall here consider two spherical coordinates referred to the $x'y'z'$-system as in the preceding section, and the $\bar{x}\bar{y}\bar{z}$-system having a common origin with the former. The latter is taken in such a way that each of them is parallel to each exis of the xyz-system. When the angles, Θ', Φ' etc. are measured as indicated in Fig. 5, we get, $x'=r\cos\Theta'\cos\Phi'=r\cos\eta$, $z'=r\sin\Theta'$ and $\bar{x}=r\cos\Theta\cos\Phi$, $\bar{z}=r\sin\Theta$. From the relation between the two systems: $x'=\bar{x}\cos\theta+\bar{z}\sin\theta$, η can be connected with Θ and Φ as follows:

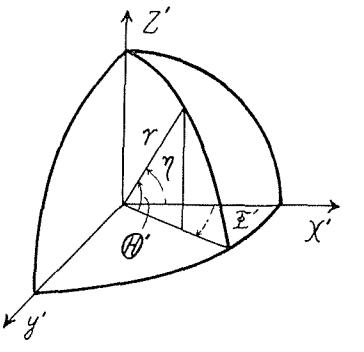

Fig. 5.

$$\cos\eta = \cos\Theta'\cos\Phi' = \cos\Theta\cos\Phi\cos\theta+\sin\Theta\sin\theta\,. \qquad (14)$$

For the xyz-system, we have

$$x = \Delta\cos\Theta\cos\Phi\,,\quad h = \Delta\sin\Theta\,,\quad (\Delta^2 = x^2+y^2+h^2)\,,$$

Δ being the hypocentral distance.

When elastic waves emitted from a focus are propagated in the form of spherical

waves, their divergence factor of amplitude is found to be $1/\Delta$. Taking account of this factor, the amplitudes of the initial P- and S-waves, A_P and A_S, which will be observed at a distant station on the Earth's surface, are expressible by the following formulae, under the assumption of uniform medium:

$$A_P = \frac{2A_{P0}}{\Delta}\left[(\cos\Theta\cos\Phi\cos\theta + \sin\Theta\sin\theta)^2 - \cos^2\alpha\right] \tag{15}$$

$$= \frac{2A_{P0}}{\Delta}\left[\left(\frac{x\cos\theta + h\sin\theta}{\Delta}\right)^2 - \cos^2\alpha\right], \tag{16}$$

$$A_S = \frac{A_{S0}}{\Delta}\left(\frac{x\cos\theta + h\sin\theta}{\Delta}\right)\sqrt{1-\left(\frac{x\cos\theta + h\sin\theta}{\Delta}\right)^2}. \tag{17}$$

A_{P0} and A_{S0} depend upon the earthquake magnitude. Naturally, the nodal curves expressed by Eq. (3) are equivalent to the case of $A_P=0$ in the above formula.

While, the following relations hold between the amplitude of the incident P- or SV-waves and that with the vertical component, A_{PV} or A_{SV}, and the horizontal component, A_{PH} or A_{SH}, which will be observed on the ground surface. That is,

$$\left.\begin{aligned} A_{PV}/A_P &= f_P(i_P), \quad A_{PH}/A_P = g_P(i_P), \\ A_{SV}/A_S &= f_S(i_S), \quad A_{SH}/A_S = g_S(i_S), \end{aligned}\right\} \tag{18}$$

where i_P and i_S are the incident angles of the P- and SV-waves respectively. Since values of these functions have already been calculated in terms of Poisson's ratio (**24**, **25**), the amplitudes which will be recorded on the surface can be estimated excepting A_{P0} and A_{S0}.

a) Then, the ratio of the vertical component of theoretical amplitude of the P-waves at any station to that at a standard observatory is given by

$$\frac{A_{PV(j)}}{A_{PV(0)}} = \left(\frac{f_P(i_j)/\Delta_j}{f_P(i_0)/\Delta_0}\right)\cdot\frac{(x_j\cos\theta + h\sin\theta)^2/\Delta_j^2 - \cos^2\alpha}{(x_0\cos\theta + h\sin\theta)^2/\Delta_0^2 - \cos^2\alpha}. \tag{19}$$

b) The ratio of the vertical components of theoretical amplitudes of the P- and SV-waves at each station is,

$$\frac{A_{SV}}{A_{PV}} = \frac{f_S(i_j)}{f_P(i_j)}\cdot\frac{k\sin\eta_j\cos\eta_j}{\cos^2\eta_j^2 - \cos^2\alpha}. \tag{20}$$

We can easily calculate the above ratios, when h, $f_{P,S}(i_j)$ and Δ_j were estimated from the determination of hypocentre, and α, θ and x_j from the push-pull distribution of initial waves.

Table 2 gives the theoretical amplitudes of the P- and SV-waves or their ratios calculated for every earthquake, and the corresponding observed values at respective observatories. The angle of incidence was calculated by $\cos i = h/\Delta$ ($i=i_P=i_S$). The observed value corresponding to Eq. (20) was taken by the amplitudes' ratio of initial

Table 2. Theoretical and observed amplitudes.

No.	St.	Δ_j (km)	i_j	$f_p(i)$	$f_s(i)$	A_{PV}/A_{P0} ×100 (C)	A_{PV}/A_{P0} ×100 (Q)	$\bar{A}_{PV}$ (mm)	$\lvert A_{SV}/A_{PV}\rvert$ (C)	$\lvert A_{SV}/A_{PV}\rvert$ (Q)	$\lvert \bar{A}_{SV}/\bar{A}_{PV}\rvert$
201	I	28.6	69°	0.79	0.92	1.45		1.40	0.68		(0.72)
	K	23.1	64	0.91		1.82		2.30			
	N	25.6	66	1.74		1.92		1.40			
	Y	21.3	61	0.97	1.12			5.05	1.42		(1.32)
207	K	4.9	44	1.39	1.48	6.36		3.60	0.91		0.42
	N	9.5	68	1.73		−5.97		− 2.10			
	Y	7.8	63	0.94	1.08	−3.09		− 1.20	2.25		1.75
217	W	8.0	7	1.97				2.05			
	F	9.5	34	1.61	0.90	1.17		22.0	2.17		(2.83)
	K	11.3	41	1.46	1.57	−0.05		− 3.55	20.3		(18.1)
	N	14.8	58	1.72		0.11		11.15			
	Y	12.0	49	1.26				1.35			
218	I	9.5	54	1.15	1.23	−0.23	− 1.75	− 0.60	19.3	6.86	19.4
	W	7.5	42	1.43	1.52	2.16	2.49	2.90	0.55	0.20	0.69
	F	6.8	35	1.57	0.48	1.48	12.55	2.80	0.51	0.45	1.90
	K	6.3	27	1.74	0.95	0.22	5.43	0.70	21.4	0.10	(12.3)
	N	11.1	59	1.74		1.69		3.85			
220	I	5.1	8	1.97	0.38			2.35	0.53		(2.72)
	W	9.0	55	1.11	1.22	−2.62		− 2.10	2.49		1.33
	F	6.2	35	1.49	0.48	0.89		1.65	4.22		(3.53)
	K	8.3	52	1.20	1.28			1.00	0.73		(1.81)
	N	8.0	50	1.62		2.86		3.15			
	Y	13.3	67	0.82	0.98	0.41		0.80	8.80		(10.7)
223	I	9.2	56	1.10	1.20	0.41	2.73	0.60	10.4	2.22	(14.4)
	W	6.3	36	1.57	0.60	6.26	17.85	3.05	0.65	0.36	0.39
	N	11.4	63	1.75		3.13		3.80			
	Y	7.4	46	1.35	1.42	6.01	0.40	7.45	1.59		(1.71)
226	I	16.1	62	0.95	1.10	−1.31	− 1.92	− 1.50	2.54	1.74	3.10
	W	13.3	56	1.10	1.20	−3.51	− 0.38	− 2.05	1.25	2.53	0.80
	F	13.2	58	1.11	1.17	−1.07	− 1.66	− 2.75	3.39	1.61	(1.70)
	K	10.9	47	1.31		−0.87	− 6.12	− 4.15			
	N	16.0	63	1.75				8.85			
	Y	8.0	22	1.83	0.82	1.97	5.12	3.25	1.37	0.05	(0.92)
228	I	12.5	55	1.13	1.22	1.47		0.70	2.74		1.79
	W	7.9	23	1.81	0.84	8.95		5.40	0.01		0.48
	F	10.3	46	1.35		4.16		1.25			
	N	16.5	64	1.75		2.81		1.45			
	Y	12.6	55	1.13	1.21	1.29		1.00	3.19		1.90
230	I	11.2	42	1.44	1.53	−2.39	− 4.27	− 0.95	2.19	0.12	(2.04)
	W	8.4	3	1.99	0.18	0.42	8.68	0.70	1.12	0.22	3.14
	F	9.3	25	1.79	0.90	−0.11	− 2.66	− 1.15			
	N	14.2	54	1.67		0.24		1.80			
236	W	12.4	59	1.01	1.17	2.28	7.89	0.70	0.13	3.00	
	K	10.9	55	1.13	1.22	−0.48	− 1.75	− 0.50	14.4	1.69	1.14
	N	16.7	68	1.73		−2.02		− 3.45			(15.8)
	Y	6.8	23	1.83	0.84	6.63		17.50	0.42	0.79	(1.15)
247	I	30.9	67	0.83	1.00	0.91		8.50	2.51		1.41
	W	30.1	67	0.84		1.60		4.25			
	F	28.9	66	0.87		1.31		13.40			
	K	25.4	62	0.96		1.61		8.30			
	N	28.2	65	1.75		1.15		10.00			
	Y	23.1	59	1.03	1.16	2.44		19.00	0.90		(0.85)
248	I	7.5	53	1.18	1.25	−1.02	− 9.20	− 0.60	6.65	1.41	5.60
	W	5.0	24	1.79	0.87	6.44	9.50	1.60	0.95	1.47	0.81
	N	11.2	66	1.74		1.94		1.40			
249	I	10.5	33	1.62	0.97	−0.54		− 0.55	5.00		(6.25)
	W	9.3	19	1.87	0.72	3.22		1.10	1.10		3.68
	N	13.3	50	1.62		1.23		1.50			
250	I	7.6	61	0.99		−1.51		− 0.50			
	F	4.6	37	1.55	1.58	1.04		0.80	11.7		(13.2)
	N	9.7	68	1.73		1.23		1.60			
251	F	10.4	60	1.01	1.14	6.23		1.05	0.72		0.92
	N	13.9	67	1.74		9.20		3.10			
253	I	8.5	39	1.49	1.60	1.12		1.40	7.94		(6.00)
	W	8.6	40	1.48	1.58	2.47		1.80	3.69		(5.00)

Δ_j: the hypocentral distance; i_j: the angle of incidence; $f_P(i_j)$, $f_S(i_j)$: the ratio of the amplitude observed on the ground surface to the one of incident P- and SV-waves, respectively, A_{PV}, $\bar{A}_{PV}$: the vertical components of theoretical and observed amplitudes of P-waves respectively, A_{SV}, $\bar{A}_{SV}$: the vertical components of theoretical and observed amplitudes of SV-waves respectively, (C): the case of conical type, (Q): the case of quadrant type.

P- and *SV*-waves in the case of clear commencement of *S*-waves, otherwise by the maximum amplitudes' ratio of both waves. In this calculation the ratios for the stations near nodal curves were excluded on account of their great uncertainty.

Moreover, Eq. (19) does not include the quantity relating to the magnitude of earthquake. It is therefore possible to study by superposing the relationships between the theoretical and observed amplitude ratios for all of these earthquakes, if all shocks were caused by the same mechanism of occurrence.

This relation for the *P*-waves is shown in Figs. 6 and 7, taking Wakanoura and

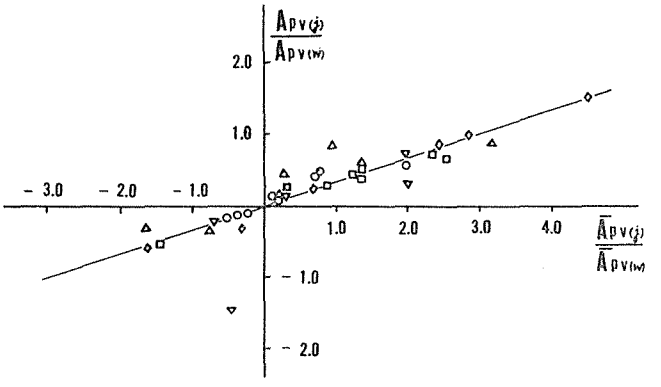

Fig. 6.

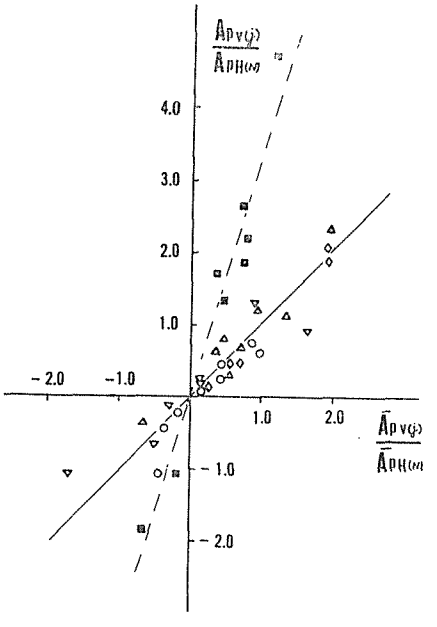

Fig. 7.

Amplitudes' ratios of initial *P*-waves between any station and a standard one in case of conical type. (ordinate: theoretical ratio, abscissa: observed ratio)

○: I, △: F, ▽: K, ◇: Y, □, ▩: N-W

Nokami as the standard station respectively. The calculated errors in these ratios are illustrated in Fig. 8. In the former figures the mean values were adopted.

Provided that all assumptions thus far made are correct and that the "ground-coefficient" (which is defined only in this case as a factor of amplification effect of the ground or a stational correction, not included in Eq. (17)) and the response of seismometer used are the same in all stations, the plotted points indicating the above relation are expected to lie on the 45°-line. It can be said that in Fig. 6 these points lie on a certain straight line with satisfactory accuracy, but its gradient is less than 45°. This fact is considered to indicate that the amplitudes observed at Wakanoura are always smaller than the values expected from the theory throughout all shocks but the ground coefficients at another five stations are nearly equal. This can be ascertained also in Fig. 7 from the steeply inclined line indicating $A_{PV(W)}/A_{PH(N)}$ and the line of 45°-gradient relating to the other stations. The coefficient at Wakanoura is estimated to be about one third of that at other stations. This is reasonably explained from the fact that the station at Wakanoura is situated on a hill composed of solid rock (crystalline schist).

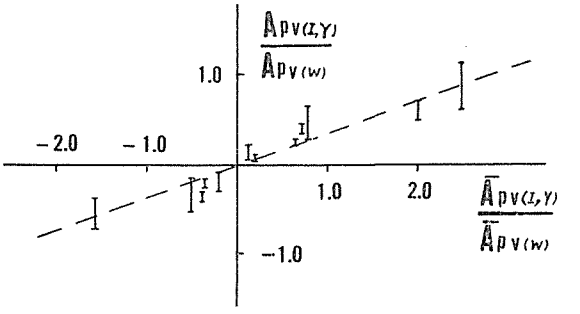

Fig. 8. Amplitude-ratios with calculated errors.

As can also be seen in Fig. 9, the observed amplitude-ratios of the P- and SV-waves may be in fairly good accord with the theoretical ratios.

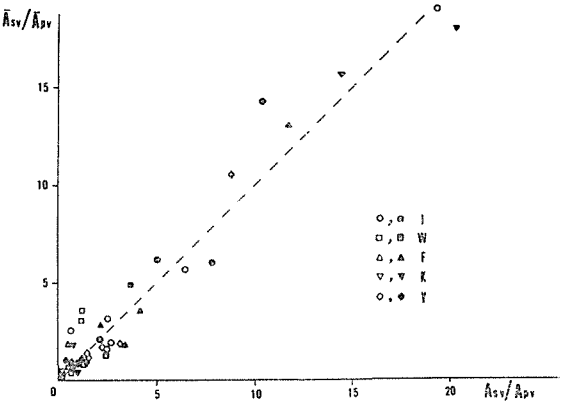

Fig. 9. Theoretical and observed amplitude-ratios of P- and SV-waves at the respective stations in case of conical type. (abscissa: theoretical ratio, ordinate: observed ratio)
Empty symbols denote the initial amplitude-ratios, and filled symbols indicate the maximum amplitude-ratios.

Taking these circumstances into consideration, we may safely consider that the mechanism of local eathquakes in this district is explainable to be of a conical type.

6. Comparison of amplitude distributions in the two types

For the sake of comparison, the theoretical amplitudes in the selected several

shocks were here estimated, assuming the push-pull distribution to be of a quadrant type.

The vertical amplitudes of the P- and SV-waves, which will be recorded on the ground surface, can be expressed, after H. Honda (**17, 26**), as follows:

$$\left.\begin{aligned} A_{PV} &= A_{P0} f_P(i_P) \sin 2\theta \cos\varphi\,, \\ A_{SV} &= A_{S0} f_S(i_S) \cos 2\theta \cos\varphi\,, \end{aligned}\right\} \tag{21}$$

where θ and φ are spherical coordinates taking a hypocentre as the origin.

Determining the distance between the epicentre and the point of intersection of nodal curves on the surface, the inclination and orientation of the polar axis (the intersection of two nodal planes), and hence, θ and φ can be obtained. The theoretical values calculated by Eq. (21) are also given in Table 2. Figs. 10 and 11 illustrate the relation between the theoretical and observed amplitudes analogously to Figs. 6 and 7.

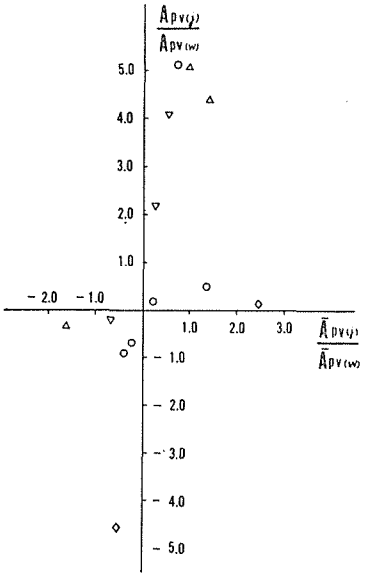

Fig. 10. Amplitudes' ratios of initial P-waves between any station and a standard one in case of a quadrant type.

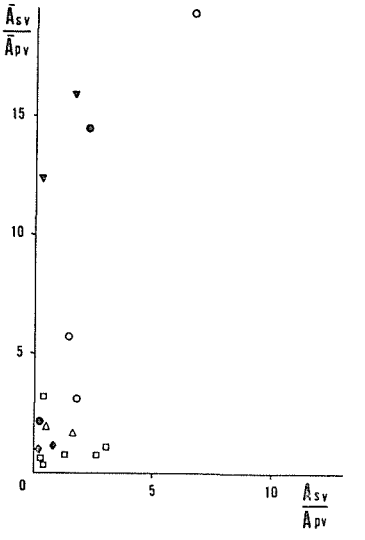

Fig. 11. Theoretical and observed amplitude ratios of P- and SV-waves in case of quadrant type.

Comparing the corresponding figures in the two types with each other, it is found that the plotted points in the case of the conical type scatter less widely than those in the case of the quadrant type. As a matter of course, it is dangerous to deny, from these results alone, a possibility of the latter type in the present case, owing to the poorer data and considerable ambiguity in the determination of nodal curves. However,

the former type of mechanism may be considered to give a more natural explanation for our observed results.

7. Some considerations

The generation mechanism of local shocks treated here can substantially be explained to be of a conical type, as described in the preceding sections. Hence in this section, some considerations will be made on this type of mechanism.

(1) Distribution of nodal cones.

In one of the studies on micro-earthquakes, the push-pull distribution of initial motions in many shocks was found to be identical with each other and similar to the main shock (**6**). However, this tendency could not be recognized in our observations.

Here, the distributions of some kinds of quantities about the nodal cone are briefly discussed in the following.

a) The frequency distribution of the half vertical angle of the cone, α, is shown in Fig. 12. For most of the earthquakes, it is found to be from 60° to 70°. The spectrum indicated in Fig. 12 seems to resemble a Gaussian distribution.

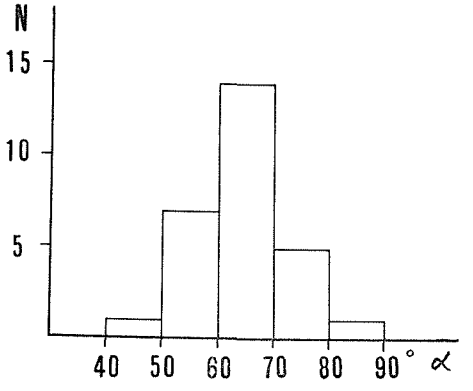

Fig. 12. Frequency distribution of α.

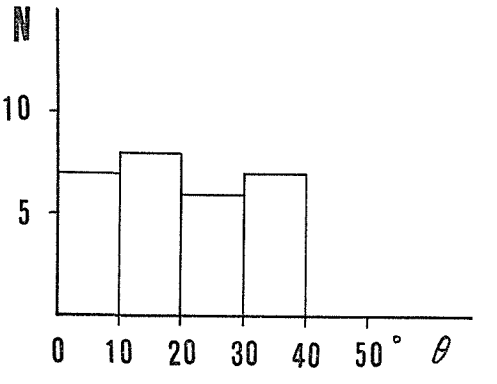

Fig. 13. Frequency distribution of θ.

b) Fig. 13 shows the histogram of the inclined angle to the ground surface, θ, of the conical axis. It seems in our case that the distribution of θ is limited within the range from 0° to 40°. We could not definitely find out the case in which the axis is so inclined that the nodal curve came to an ellipse. This agrees with Fukutomi's result (**27**), in which nodal curves were represented by a hyperbola for most of shallow earthquakes with focal depth from 0 to 25 km.

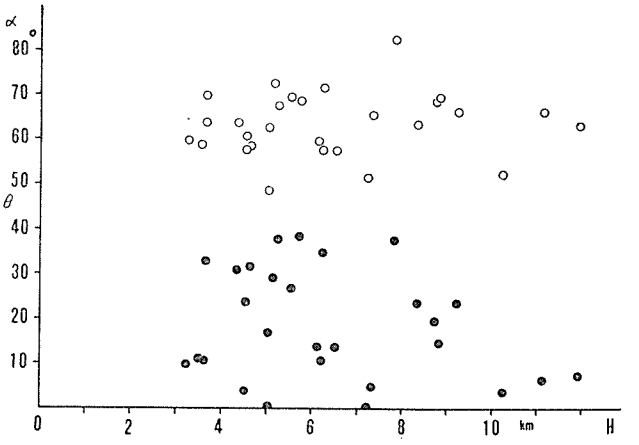

Fig. 14. Distributions of α and θ *versus* focal depth.

c) In Fig. 14, α and θ are plotted against the focal depth. No clear relation between them is recognizable.

d) Fig. 15 gives the geographical distribution for axial orientations of nodal cones. The arrows indicate the upward direction of the conical axis. They can be regarded neither to distribute systematically nor to relate with directions of geological faults, though some investigations (**9, 10**) showed a relation between the direction of faults and the pattern of initial waves in certain local earthquakes.

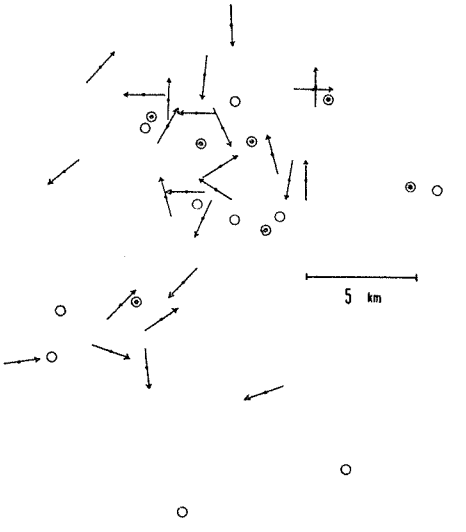

Fig. 15. Geographical distribution of axial orientations of nodal cones.

(*2*) *A consideration on the origin of local shocks in this area*

Here, we shall tentatively make a consideration about the mechanism of earthquake occurrence with a conical type distribution.

The difference in travel times concerning the push and pull of initial motions (**11**), which was detected in our observations, may be considered to suggest an azimuthal difference in the generation mechanism or the shape of focal region. On the other hand, in the present research on the push-pull distribution, we find 16 nodal cones with push-sense inside and 12 cases with pull-sense inside. In all of these

cases, the observation stations inside the nodal cone are found to belong to the group with the earlier arrival of the two, which were classified by their travel times. We can imagine from these reasons that the focal domain may have a longer dimension in the direction of conical axis, if anisotropy is permissible in the hypocentral form.

To such a model of origin which has the above-mentioned shape of hypocentre and the mechanism of conical type, Usami's hypothetical focus (prolate spheroidal cavity in an infinite elastic medium) may be considered to correspond. He confirmed in his model that a push-pull distribution of conical type took place in the following three cases: i) $a/b=3$, $\lambda/2c=\pi/3$, ($\alpha=66°$), ii) $a/b=\infty$, $\lambda/2c=\pi$, ($\alpha=42°$), iii) $a/b=\infty$, $\lambda/2c=\infty$, ($\alpha=55°$), where a, b and c are the longer and shorter axes and the focal distance of the spheroid respectively and λ is the wavelength. The general relationship between the wavelength and the angle of vertex of nodal cone was not solved by him, but he elucidated that the latter is functionally related to $\lambda/2c$ with a/b as a parameter. It is probably admissible, however, to consider from his results that α may increase with the increase of $\lambda/2c$ under the constancy of a/b.

With a view to examine whether the disparity in travel times between two groups comes from the azimuthal difference of focal form or not, the relation between the vertical angle of nodal cone, α, and the time-difference, δT, was investigated. In Fig. 16, the observed values of α are plotted against $2t_0/\delta T$ instead of $\lambda/2c$. t_0 is

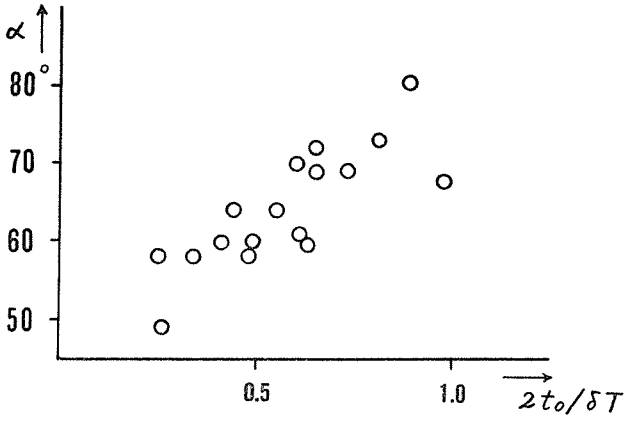

Fig. 16. Relation between vertical angle of nodal cone and period of initial waves.

the original half-period of initial P-waves radiated from the focus. It cannot be easily estimated by extrapolation of the previously determined relation (28) between the initial period and hypocentral distance, so that in this case it was substituted for the half-period of initial motion observed at the nearest station to the focus. From this figure, it can be recognized that α tends to increase remarkably with the increase

in $2t_0/\delta T$. Consequently, the travel-time difference between two groups may safely be interpreted to come from the azimuthal difference in the focal shape, though some questions remain unsolved. It may also be said that the present result has added a more possible ground to regard the shape of hypocentral domain as an approximate spheroid or linear source, as far as the present case is concerned.

If a general relationship between the vertical angle of nodal cone and the ratio of the wavelength to the dimension of origin is established, we shall obtain more definite informations about the dimension of focal region.

8. Conclusion

For the purpose of clarifying the mechanism of occurrence in micro-earthquakes, the push-pull pattern of initial motions and the amplitude distribution of the *P*- and *S*-waves was studied for a great number of local shocks generated in Wakayama District.

(1) The geographical pattern of the initial waves indicates a systematic distribution, but it is difficult to judge exactly, solely from the distribution, whether the mechanism is of a quadrant type or of a conical type. There seems to be many cases corresponding rather to the latter type.

(2) The distributions of theoretical amplitudes of the *P*- and *S*-waves in both types were calculated and compared with the observed values at each station. They are in fairly good accord with each other in the case of a conical type, while a larger discrepancy was found in a quadrant type. This fact may be considered to indicate that the mechanism of local earthquakes in this region can be explained to be of a conical type.

The amplitudes observed at Wakanoura are in a constant ratio smaller than the values expected from the theory. This is accepted by the reason that the station is situated on a hill composed of harder rock.

(3) On the basis of this result, the angle of vertex of nodal cone and the inclination angle of conical axis were estimated for all of the shocks. For the greater part of them a half-angle of the former was found to be $60°\sim70°$, and its frequency distribution is similar to a Gaussian distribution. The latter is distributed over $0°\sim40°$. Both of them do not seem to be related with the focal depth. No systematic pattern was recognizable in the geographical distribution of the orientations of conical axis.

(4) Some considerations were made on the origin of these shocks. A certain relationship seems to hold between the vertical angle of the nodal cone and the period of initial waves. It is probably possible to presume from this result that the focal region may have an azimuthal difference in its shape.

Acknowledgements

The writer wishes to express his cordial thanks to Prof. E. Nishimura for his kind guidance, and to Prof. K. Sassa for his instructive advice. Many thanks are also due to Mr. M. Ōtsuka, Dr. T. Nishitake and Mr. A. Kamitsuki for their valuable suggestions, and to Mr. K. Mori for drawing figures. The author is greatly indebted to the data obtained at the stations of the Earthquake Research Institute.

The expense for this study was partly defrayed by a grant-in-aid for scientific researches of the Ministry of Education.

REFERENCES

1. H. KAWASUMI, A historical sketch of the development of knowledge concerning the initial motion of earthquake, Bur. Centr. Seism., Travaux Scientifique **15** (1937), 1.
2. H. HONDA, The mechanism of the earthquakes, Sci. Rep. Tohoku Univ., [5], **9** (1957).
3. K. KASAHARA, The natures of seismic origins as inferred from seismological and geodetic observations (2), Bull. Earthq. Res. Inst., **36** (1958), 21.
4. P. BYERLY, Natures of faulting as deduced from seismograms, Geol. Soc. America, Special Paper, **62** (1955), 762.
5. J. H. HODGSON, *Natures of faulting in large earthquakes*, Bull. Geol. Soc. America, **68** (1957), 611.
6. H. HONDA, On the mechanism and types of the seismograms of shallow earthquakes, Geophys. Mag., **5** (1932), 69.
7. B. GUTENBERG, Mechanism of faulting in southern California indicated by seismograms, Bull. Seism. Soc. America, **31** (1941), 263.
8. P. G. GANE, P. SELIGMAN and J. H. STEPHEN, Focal depths of Witwatersland tremors, Bull. Seism. Soc. America, **42** (1952), 239.
9. S. OMOTE, On the aftershocks of the Fukui Earthquake, Bull. Earthq. Res. Inst., **28** (1950), 311.
10. S. OMOTE, Aftershocks of Imaichi Earthquake observed at Nishi-oashi station, Bull. Earthq. Res. Inst., 28 (1950), 401.
11. T. MIKUMO, Precise seismometric observations in the epicentral region of local shocks, Mem. Coll. Sci. Kyoto Univ., A28 (1956), 161.
12. M. ISHIMOTO, Existence d'une source quadruple au foyer sismique d'après l'étude de la distribution des mouvements initiaux des secousses sismique, Bull. Earthq. Res. Inst., **10** (1932), 449.
13. H. KAWASUMI, Study on the propagation of seismic waves (2nd Paper), Bull. Earthq. Res. Inst., **11** (1933), 403; **12** (1934), 660.
14. K. SEZAWA, Dilatational and distortional waves generated from a cylindrical or a spheroidal origin, Bull. Earthq. Res. Inst., **2** (1927), 13.
15. T. MATUZAWA, On the relative magnitude of the preliminary and the principal portion of earthquake motions, Jap. J. Astr. & Geophys., **4** (1926), 1.
16. M. HASEGAWA, Die erste Bewegung bei einem Erdbeben, Beitr. z. Geophys., **27** (1930), 102.
17. H. HONDA, On the amplitude of the *P* and *S* waves of deep earthquakes, Geophys. Mag., 8 (1934), 153.
18. W. INOUYE, Notes on the origin of earthquake, Bull. Earthq. Res. Inst., **14** (1936), 582; **15** (1937), 956.
19. S. TAKAGI, On the origin of earthquake (2), (3), (4), Quart. J. Seism., C.M.O., **14**-3 (1950), 1; **17**-3 (1953), 53; **17**-4 (1953), 1 (in Japanese).

20. T. HIRONO and T. USAMI, Stress in an infinite medium around a spheroidal cavity applied with hydrostatic pressure, Pap. in Met. & Geophys., **5** (1954), 64.
21. T. USAMI and H. HIRONO, Elastic waves from a spheroidal cavity whose wall is subjected to normal stress of harmonic type, Pap. in Met. & Geophys., **7** (1956), 287; Geophys. **29** (1958), 11.
22. T. MINAKAMI, Distribution des mouvements initiaux d'un séisme dont le foyer se trouve dans la couche superficielle et détermination de l'épaisseur de cette couche, Bull. Earthq. Res. Inst., **13** (1935), 114.
23. S. TAKAGI, On the origin of earthquake (10), Quart. J. Seism., C.M.O., **18-2** (1953), 52 (in Japanese).
24. T. MATUZAWA, An example in case of surface reflection of plane waves J. Seism. Soc., Japan, **3** (1932), 7 (in Japanese).
25. L. KNOPOFF, R. W. FREDRICKS, A. F. GANGI and L. D. PORTER, Surface amplitudes of reflected body waves, Geophys., **22** (1957), 842.
26. H. HONDA and H. ITŌ, On the reflected waves from deep focus earthquakes, Sci. Rep. Tôhoku Univ., **3** (1951), 144.
27. T. FUKUTOMI, Some statistical problems concerning intial earthquake motion, Bull. Earthq. Res. Inst., **11** (1933), 510.
28. T. MIKUMO, On the periods of seismic waves observed in local earthquakes, Mem. Coll. Sci., Kyoto Univ., A**29** (1958), 1.